Journal of Assisted Reproduction and Genetics (2022) 39:107–116
https://doi.org/10.1007/s10815-021-02330-x

EMBRYO BIOLOGY

The function of Nucleoporin 37 on mouse oocyte maturation and preimplantation embryo development

Qianying Guo[1,2,3,4,5] · Qiang Liu[1,2,3,4,5] · Nan Wang[1,2,3,4,5] · Jing Wang[1,2,3,4,5] · Andi Sun[1,2,3,4,5] · Jie Qiao[1,2,3,4,5] · Liying Yan[1,2,3,4,5]

Received: 19 May 2021 / Accepted: 20 September 2021 / Published online: 13 January 2022

Abstract

Purpose Nucleoporin 37 (NUP37) has been reported to activate the YAP-TEAD signaling, which is crucial for early embryo development. However, whether NUP37 is involved in oocyte meiosis and embryo development remains largely unknown. The study aimed to clarify the function of *Nup37* in oocyte maturation and early embryo development, and to explore the mechanism.

Methods The expression level and subcellular localization of NUP37 were explored. After knocking down of *Nup37* by microinjecting interfering RNA (siRNA), the oocyte maturation rate, aberrant PB1 extrusion rate, and blastocyst formation rate were evaluated. In addition, the effect of the downregulation of *Nup37* on YAP-TEAD signaling was confirmed by immunofluorescence staining and real-time quantitative PCR.

Results NUP37 was highly expressed in oocytes and early embryos; it mainly localized to the nuclear periphery at mice GV stage oocytes and early embryos. *Nup37* depletion led to aberrant PB1 extrusion at the MII stage oocyte and a decreased blastocyst formation rate. The reduction of NUP37 caused YAP1 mislocalization and decreased the expression of *Tead1*, *Tead2*, and *Tead4* during mice embryo development, thus affecting the YAP-TEAD activity and embryo developmental competence.

Conclusions In summary, NUP37 played an important role in mice oocyte maturation and preimplantation embryo development.

Keywords Nucleoporin 37 · YAP-TEAD · Oocyte maturation · Blastocyst formation · Nuclear pore complexes

Introduction

The nuclear pore complex (NPC) is assembled by ~ 30 different proteins called nucleoporins (NUPs) and serves as the gatekeeper of the nucleus [1–3]. The main function of NPCs is to control the nucleocytoplasmic transport (NCT) of RNAs and proteins, as well as participate in many other cellular processes, such as chromosome segregation and genome stabilization [4–6]. NPCs also play an important role in fertility. NUP35 and ALADIN, another member of NPC, are involved in spindle assembly during oocyte maturation [7, 8], and the mutation of *NUP210L* impairs male fertility [9]. Additionally, the destruction in some NUPs, such as NUP50, NUP98, and ELYS, is embryonically lethal [10–12].

According to our previous transcriptomic study, *NUP37*, as a key member of NPCs, is highly expressed in human oocytes and preimplantation embryos [13]. NUP37 and other 9 proteins (SEC13, SEH1, NUP96, NUP85, NUP107,

Qianying Guo and Qiang Liu contributed equally to this work.

✉ Liying Yan
yanliyingkind@aliyun.com

1 Center for Reproductive Medicine, Department of Obstetrics and Gynecology, Peking University Third Hospital, Beijing 100191, China

2 National Clinical Research Center for Obstetrics and Gynecology, Peking University Third Hospital, Beijing 100191, China

3 Key Laboratory of Assisted Reproduction (Peking University), Ministry of Education Beijing Key, Beijing 100191, China

4 Laboratory of Reproductive Endocrinology and Assisted Reproductive Technology, Beijing 100191, China

5 Research Units of Comprehensive Diagnosis and Treatment of Oocyte Maturation Arrest, Chinese Academy of Medical Sciences, Beijing, China

NUP160, NUP133, NUP43, and ELYS) constitute the Nup107-160 complex in metazoans [3, 14]. The spindle assembly and positioning, along with the correct connection between microtubule and chromosome, are important for both mitosis and meiosis [15, 16]. Meiosis defects during oocyte maturation lead to chromosome segregation errors and aneuploidy embryo formation [17]. Moreover, the Nup107-160 complex plays an important role in promoting spindle assembly through microtubule nucleation by interacting with γ-TuRC during mitosis [18]. However, NUP37 has not been studied in oocyte maturation (meiosis) or embryo development yet.

NUP37 promotes the progression and invasion of hepatocellular carcinoma (HCC) cells by interacting with Yes-associated protein (YAP) and activating YAP-TEAD (transcriptional enhanced associate domain) signaling [19]. YAP is a key downstream effector of the Hippo signal pathway and constantly shuttles between the cytoplasm and the nucleus. Once YAP, with an activation domain, has accumulated in the nucleus, it acts as a coactivator of TEAD, with a DNA-binding domain [20, 21]. The functions of YAP-TEAD and the Hippo signaling pathway in embryogenesis have been extensively investigated, including their role in blastocoel formation and epiblast (EPI) formation [22–25].

These clues hint that NUP37 may play a role in oocyte maturation and early embryo development, and this study aimed to elucidate the role of NUP37 in these processes and to explore the mechanisms. In this study, we found that NUP37 depletion in oocytes led to abnormal asymmetric division, and NUP37 depletion in zygote led to lower blastocyst formation rate probably by regulating YAP localization and TEAD expression in mouse embryos.

Materials and methods

Animals

ICR mice were provided by Peking University Health Science Center Department of Laboratory Animal Science (Beijing, China). Mice were reared in a temperature-controlled room (a 12-h light–dark period), with a temperature of 18–23 ℃ and 40–60% humidity, with food and water ad libitum. Animal experimental procedures were followed as the Institutional Animal Welfare and Ethics Committee policies of Peking University (LA2018261).

Oocyte and embryo collection and culture

Six- to eight-week-old female mice were intraperitoneally injected with 7.5 IU pregnant mare's serum gonadotropin (PMSG, Ningbo Second Hormone Factory) for 42–48 h; after sacrificed by cervical dislocation, cumulus-oocyte-complexes (COCs) were obtained by manually puncturing ovary follicles. Cumulus cells were removed by mouth pipette to obtain denuded germinal vesicle (GV) oocytes. M16 medium (Sigma, M7292) was used for oocyte culture. Germinal vesicle breakdown (GVBD), metaphase I (M I), and metaphase II (M II) oocytes were collected at 4 h, 8 h, and 12 h for subsequent analysis. For microinjection, GV oocytes were cultured in M2 medium (Sigma-Aldrich, M7167) with 2.5 μM milrinone (Selleckchem, S2484) to prevent meiosis resumption.

For embryo collection, 6–8-week-old female mice were intraperitoneally injected with 7.5 IU PMSG followed by 7.5 IU human chorionic gonadotrophin (hCG, Ningbo Second Hormone Factory) 46 h later. Female mice were bred with adult male mice overnight after hCG injection. The next morning, female mice with vaginal plugs were used to get zygotes. Zygotes were collected from oviducts and 0.3% hyaluronidase (Sigma, H3506) was used for cumulus cells removal. 2PN (two-pronuclear) embryos were cultured in G1-plus medium (Vitrolife) at 37 ℃ and 6% CO_2.

Microinjection

GV oocytes or zygotes were microinjected with either a mix of *Nup37* siRNAs (Ribobio) (siRNA1# 5′- CACCGTGGATTGCGAAGATTA-3′; siRNA2# 5′- ATCAAACATACTGTAAATCTA-3′; siRNA3# 5′- CCGAGGAAACTTTCAAGCTAA-3′) or non-silencing siRNA (5′-UUCUCCGAACGUGUCACGUTT-3′) as negative control (NC). The three siRNAs of *Nup37* (50 μM) were mixed equally, 5–10 pl mixture was injected into the cytoplasm of per oocyte or zygote using Eppendorf FemtoJet 4i under an inverted microscope (Nikon ECLIPSE Ti). After microinjection, GV oocytes were arrested in M2 medium containing 2.5 μM milrinone for 24 h and then cultured in M16 medium for 14 h, and zygotes were cultured in G1-plus medium directly.

Western blotting

A total number of 100 oocytes or embryos at each stage were extracted with 10 μL Laemmli Buffer (BioRad, 1,610,737). The PageRuler™ Prestained Protein Ladder (Thermo, 26,617) was used to estimate molecular weight. Proteins were separated by Sodium Dodecyl Sulfate–Polyacrylamide Gel Electrophoresis (SDS-PAGE, 10% acrylamide running gel) and transferred to polyvinylidene fluoride (PVDF) membranes (Millipore). The membranes were incubated with rabbit anti-NUP37 antibody (Abcam, ab220675, 1:100) and anti-tubulin antibody (TransGen, HC101, 1:1000) overnight at 4℃ after blocking in 5% Skim Milk (BD, 232,100). HRP-conjugated secondary antibodies (TransGen, HS201, HS101, 1:3000) were used to incubate for 2 h at room temperature after washing three times (5 min per time) in Tris-buffered

saline (10 mM Tris, 150 mM NaCl, pH 7.5) containing 0.1% Tween-20 (TBST). Chemiluminescence was detected by the ECL (Thermo, 32,106) and visualized by Tanon-5200. ImageJ (Wayne Rasband, USA) was used for analysis.

Real-time quantitative PCR (qPCR)

RNA was extracted and reverse-transcribed into cDNA from a total number of 10 oocytes or embryos as previously described [26]. qPCR analyses were performed with SYBR Master Mix (Applied Biosystems, A25742) and QuantStudio 3 Real-Time PCR System. The qPCR conditions were 95 °C for 5 min, 40 cycles of 95 °C for 30 s, 60 °C for 40 s, and 72 °C for 1 min, followed by 72 °C for 5 min. Relative gene expression was analyzed based on the $2^{-\Delta\Delta CT}$ method, and at least three independent experiments were analyzed. *Gapdh* was used as a control. The primers used in this study were designed as follows: *Nup37*: 5′- GGTGGTCGGCCA TTAGTGAAA-3′ and 5′-CCAGAACCGACAGCTACA GA-3′; *Gapdh*: 5′-GTTCCTACCCCCAATGTGTC-3′ and 5′-GTCCTCAGTGTAGCCCAAGA-3′; *Yap1*: 5′-GACTCC GAATGCAGTGTCTTC-3′ and 5′- TGTTGAGGAAGT CGTCTGGG-3′; *Tead1*: 5′-GCGGACTTAAACTGCAAT ATCC-3′ and 5′-GCTTGTGGATGAAGTTGATCATATA -3′; *Tead2*: 5′-GGCGCTTTGTGTACCGTCT-3′ and 5′-ACA CAGCAGCAGTTCCTGAGT-3′; *Tead3*: 5′-CCTCAACAG

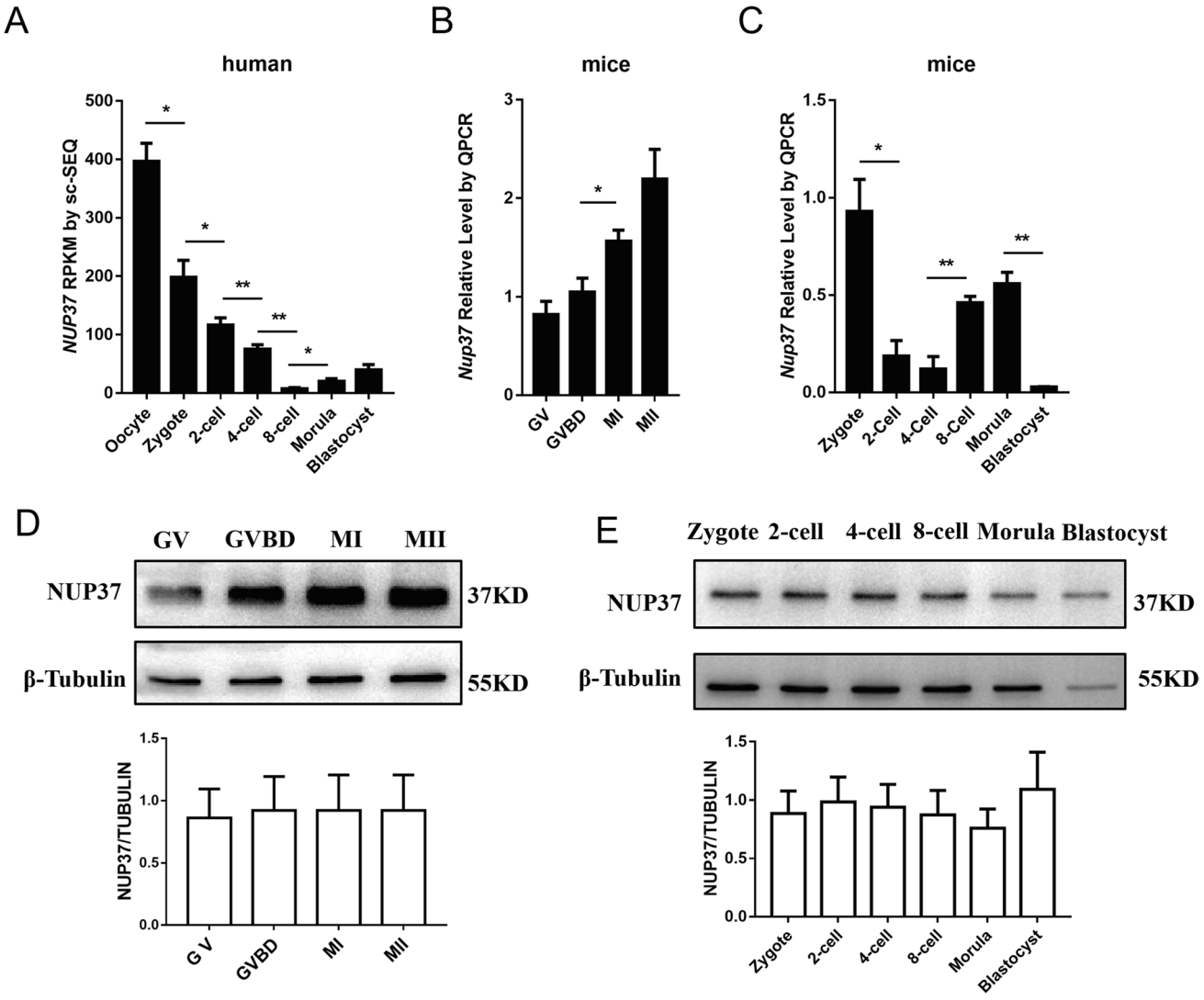

Fig. 1 Expression pattern of NUP37 during oocyte maturation and embryo development. (A) Expression of *NUP37* in human oocytes and early embryo development at single-cell resolution. Data were downloaded from a previous study [13]. RPKM, Reads Per Kilobase per Million mapped reads. (B–C) Mouse oocytes at each stage (B) and embryos from zygote stage to morula stage (C) were harvested and lysed for Western blotting. Proteins from a total of 100 oocytes or embryos were loaded for each lane, and β-Tubulin was used as control. (D–E) qPCR results showing the relative expression level of *Nup37* in mouse oocytes (D) and preimplantation embryos (E). Ten oocytes or embryos were used for each stage. Error bars indicate SEM. Independent samples *T*-test, $^{*}P < 0.05$, $^{**}P < 0.01$

CACAATCCAGG-3′ and 5′-TACTCGCACATGGGTGAGC-3′; *Tead4*: 5′-GGAGTATGCCCGCTATGAGA-3′ and 5′-TCCTGTGTGTCTCGGTTGGT-3′. The primers of *Yap1* and *Tead1-4* were as described in a previous study [27].

Immunofluorescence

Oocytes were put into the acidic solution for several seconds to remove the zona pellucida. Embryos and zona pellucida–free oocytes (10–15 oocytes or embryos at each stage for per group) were fixed in 4% paraformaldehyde (PFA) (Sigma, P6148) in PBS for 1 h, and then permeabilized with 0.3% Triton X-100 (DingGuo, DH351-2) for 30 min at room temperature. After blocking in 1% bovine serum albumin (BSA) (BioRuler, RJ0872) for 40 min, the samples were incubated with the primary antibody overnight at 4 ℃. Then, secondary antibodies (Alexa Fluor 488 goat anti-rabbit, Invitrogen, A11034, 1:200) and DAPI (10 ug/ml, Solarbio, C0065) were added to the samples for 2 h at room temperature after three washes in PBST (0.1% Tween and 0.01% Triton X-100 in PBS). Approximately 10 oocytes or embryos were mounted on a slide of glass and the images were captured by a confocal laser scanning microscope (Zeiss LSM 880). The primary antibodies were used as follows: NUP37 polyclonal antibody, ALEXA FLUOR 647-conjugated (Bioss, bs-7819R-A647, 1:100); Rabbit Polyclonal YAP1 antibody (Proteintech, 13584-1-AP, 1:100). A laser scanning confocal microscope platform (Carl Zeiss LSM 880, ZEISS, Germany) was used to take immunofluorescent photos, in which excitation light with a wavelength of 488 nm and 647 nm was used.

Chromosome spreading

Zona pellucida–free M II oocytes were washed in PBS several times and then fixed in spreading solution (1% PFA, 3 mM dithiothreitol (DTT) and 0.15% Triton X-100 in ddH_2O, pH = 9.2) on glass slides and air-dried. Chromosomes were stained with DAPI.

Statistical analysis

Statistical analysis was performed with IBM SPSS Statistics 23. Data were presented as the mean ± standard error from at least three independent replicates. The group comparisons of oocyte maturation rates, aberrant first polar body (PB1) rate, and blastocyst rate were analyzed by chi-squared test, and the comparisons of expression levels were analyzed by independent samples *T*-test. $*P < 0.05$ and $**P < 0.01$.

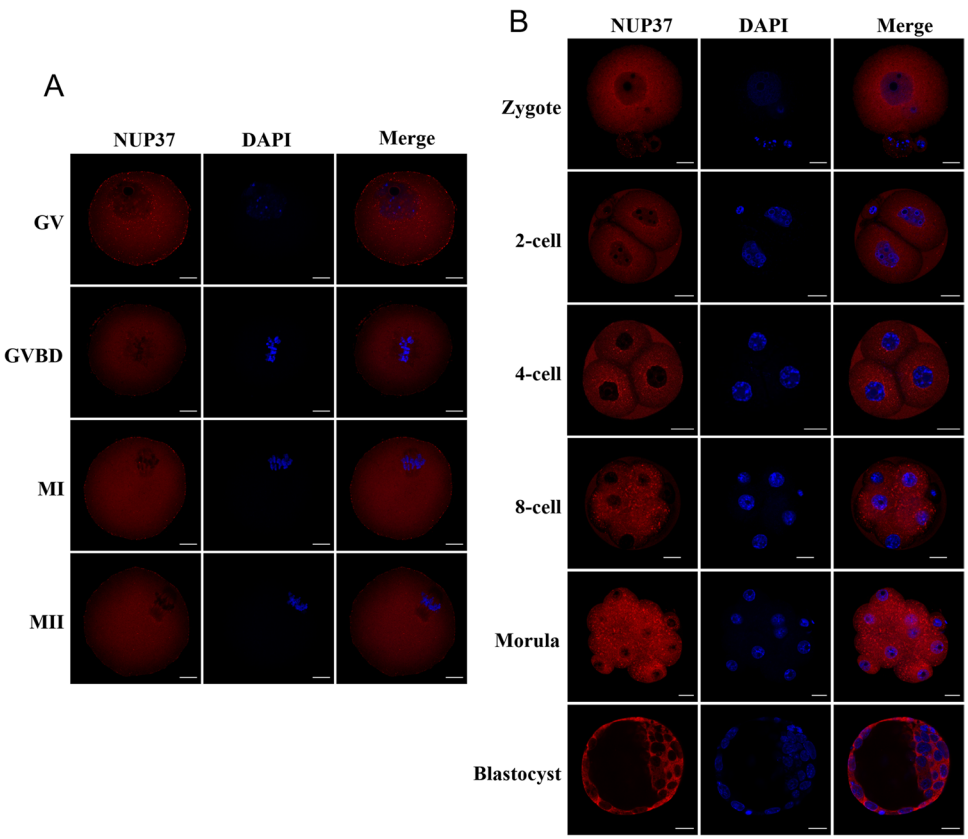

Fig. 2 Subcellular localization of NUP37 during mouse oocytes maturation and preimplantation embryo development. (A–B) Immunofluorescent staining of NUP37 at each stage of mouse oocyte maturation (A) and early embryo development (B). Scale bar, 20 μm

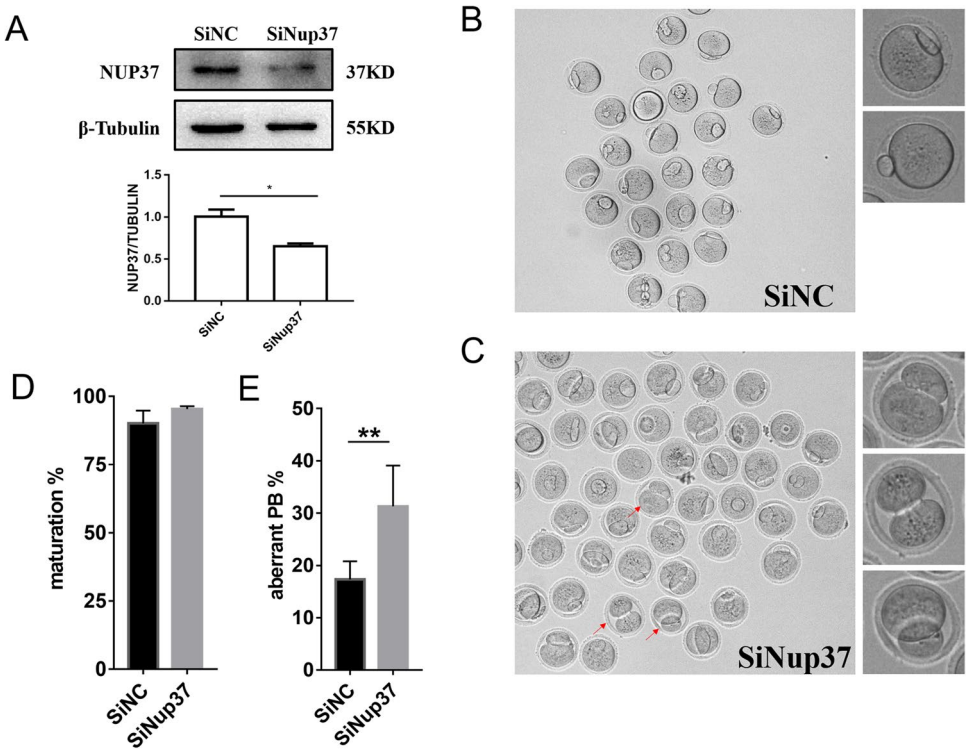

Fig. 3 Influence of NUP37 knockdown on mouse oocyte maturation. (A) Western blotting results showing reduced expression of NUP37 after injection with a mixture of *Nup37* siRNAs (SiNup37 group) compared to the Negative Control siRNA (SiNC group). Independent samples T-test, $*P<0.05$. (B–C) Representative images of oocytes in SiNC group (B) and SiNup37 group (C). Oocytes were arrested in M2 medium containing 2.5 mM milrinone for 24 h and cultured in M16 medium for another 14 h. Red arrows indicate several representative oocytes with aberrant PB1 extrusion. (D) Oocyte maturation rates of SiNup37 and SiNC. SiNC: 90.07 ± 4.67%, n = 201; SiNup37: 95.44 ± 1.01%, n = 217, $P>0.05$, Chi-Squared Test. (E) Aberrant PB1 extrusion rates of SiNup37 and SiNC. SiNC: 17.26 ± 3.51%, $n=201$; SiNup37: 31.30 ± 7.76%, $n=217$, $P<0.01$, chi-squared test. Error bars indicate SEM. $**P<0.01$

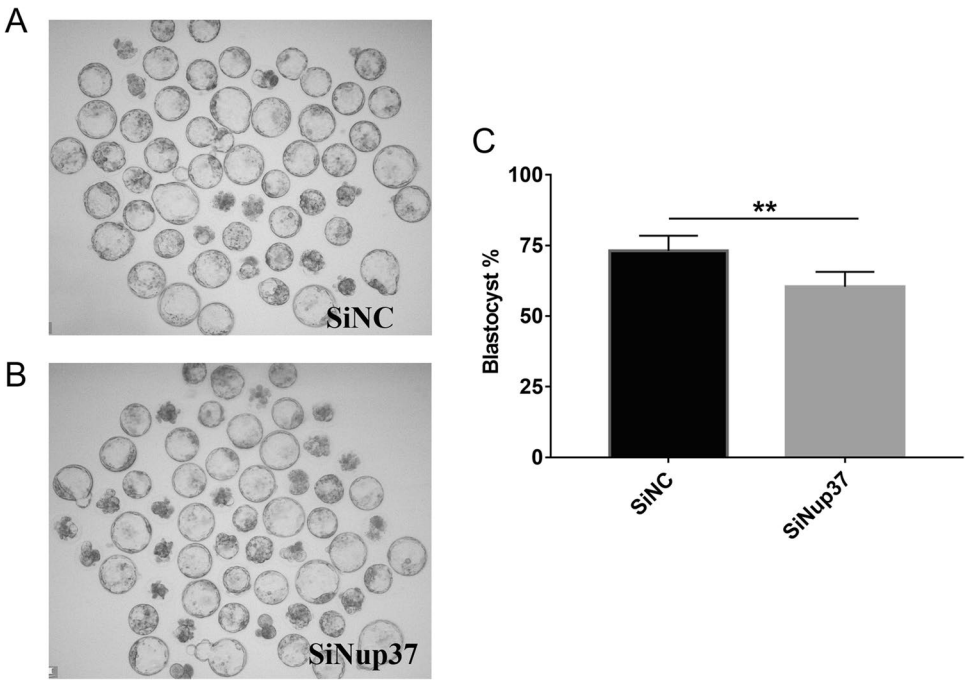

Fig. 4 Influence of NUP37 knockdown on mouse blastocyst formation. (A–B) Representative images of embryos in the SiNC group (A) and SiNup37 group (B). Embryos were microinjected with NC siRNA or a mixture of *Nup37* siRNAs at the zygote stage, and were cultured in G1-Plus medium for 4 days. (C) Blastocyst formation rate of the SiNC and the SiNup37 group. SiNC: 73.07 ± 5.37%, $n=215$; SiNup37: 60.47 ± 5.30%, $n=209$, $P<0.01$, chi-squared test. Error bars indicate SEM. $**P<0.01$

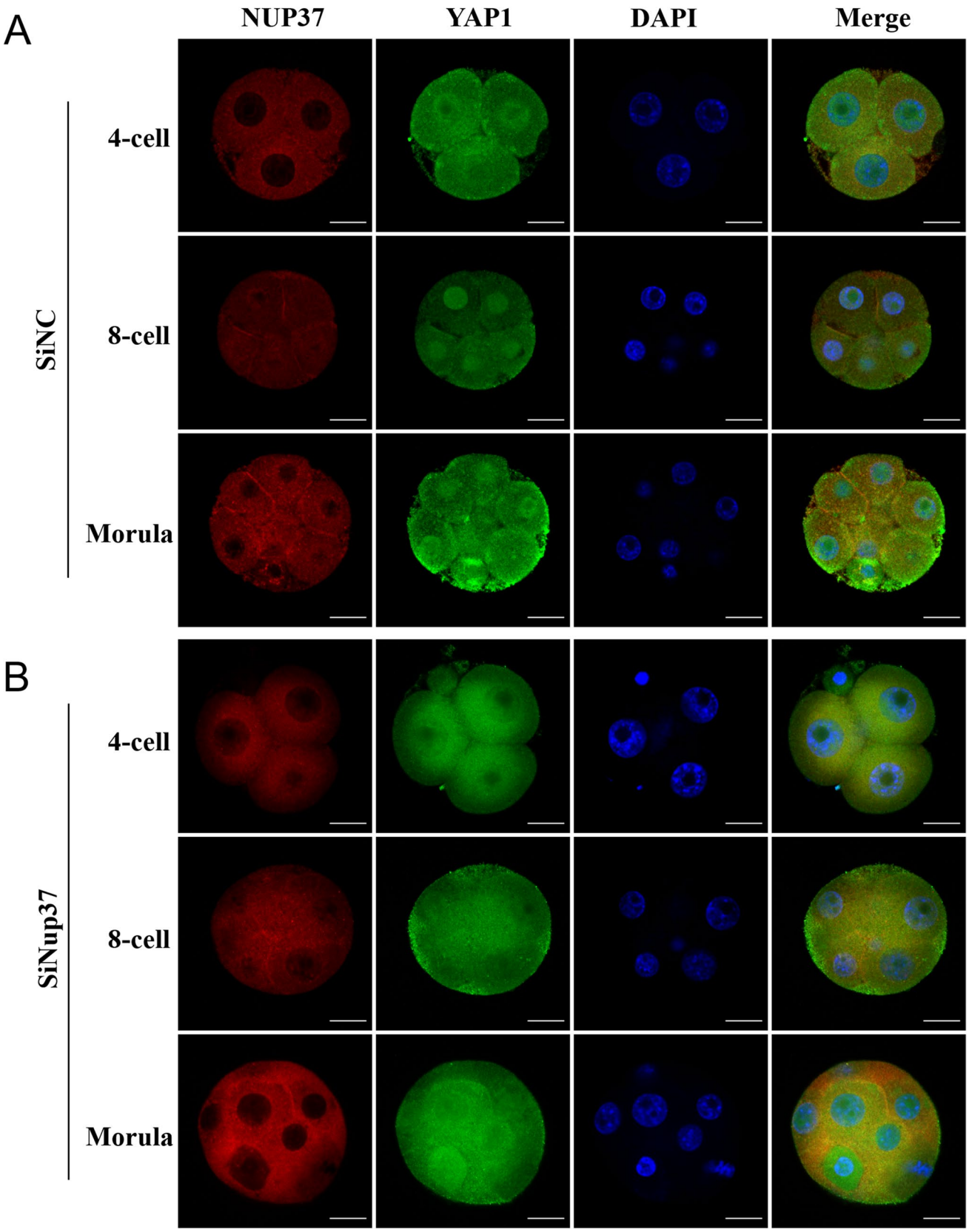
A
NUP37
YAP1
DAPI
Merge
SiNC
4-cell
8-cell
Morula
B
SiNup37
4-cell
8-cell
Morula

◂**Fig. 5** NUP37 inhibition disturbed the subcellular localization of YAP1. (A) Immunofluorescence showed YAP1 localized at the nucleus periphery of the SiNC group at the 4-cell, 8-cell, and morula stages. (B) Immunofluorescence showed YAP1 scattered throughout the whole embryos in the SiNup37 group at the 4-cell, 8-cell, and morula stages. Red, NUP37; green, YAP1; blue, DAPI. Scale bar, 20 μm

Results

NUP37 expression pattern in oocytes and preimplantation embryos

Analyzing our published RNA-seq data [13], we found that the *NUP37* expression level dramatically decreased after

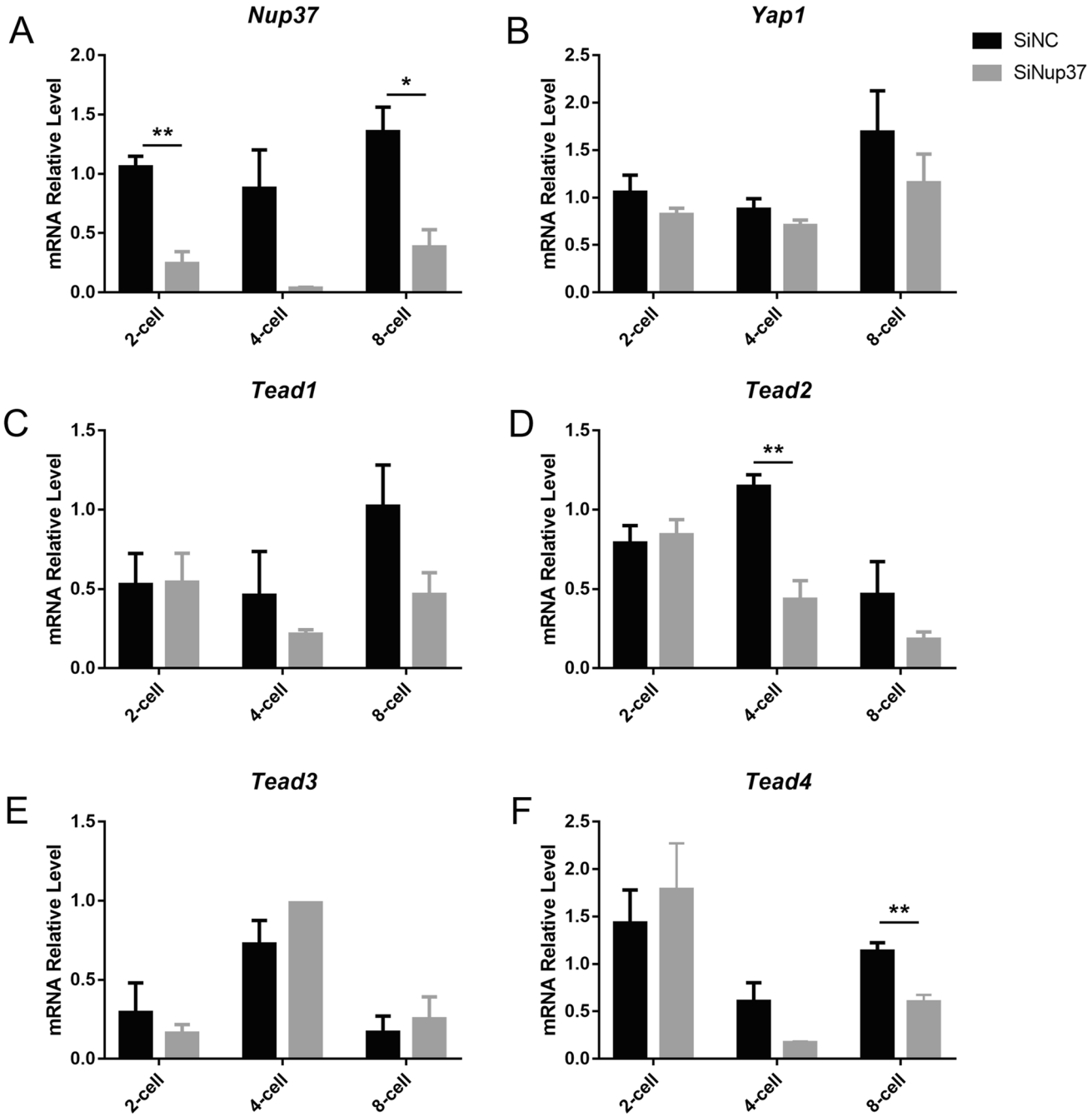

Fig. 6 Inhibition of NUP37 affected TEAD activity. (A) qPCR results verified that *Nup37* expression was reduced by different degrees. (B-F) qPCR results showing the expression changes of *Yap1* (B), *Tead1* (C), *Tead2* (D), *Tead3* (E), and *Tead4* (F) after microinjecting a mixture of *Nup37* siRNAs. $^{*}P < 0.05$, $^{**}P < 0.01$. Error bars indicate SEM

fertilization, and the zygotic transcripts gradually accumulated after zygotic genome activation (ZGA) in human (Fig. 1A). The qPCR result showed that the transcription of *Nup37* in mouse oocytes gradually increased and peaked at M II stage, whereas the Western blotting data showed barely changes in NUP37 expression. *Nup37* immediately diminished after fertilization and the zygotes started to express *Nup37* after ZGA (Fig. 1B-E). Then, we examined the subcellular location of NUP37. Results showed that NUP37 was mainly located at the nuclear periphery at GV stage, and scattered throughout the cytoplasm without specific localization after GVBD (Fig. 2A). During mouse embryo preimplantation development, NUP37 was mainly located in the nuclear periphery (Fig. 2B), and localized in the nucleus of some blastomeres at the 8-cell stage occasionally (~16%) (Figure S1).

Influences of NUP37 depletion during mouse oocyte maturation

To study the function of NUP37 in oocyte maturation, we injected a mixture of *Nup37* siRNAs into fully-grown GV stage oocytes (SiNup37 group). The NC siRNA was injected as control (SiNC group). The knockdown efficiency was verified by Western blotting (Fig. 3A). The oocyte maturation rate and the aberrant PB1 rate were calculated. PB1 with a diameter greater than 1/3 oocyte diameter was defined as abnormal. We found that there was no significant difference in maturation rate between the SiNup37 group and the SiNC group, but the aberrant PB1 rate of the SiNup37 group was significantly higher than that in the SiNC group ($P < 0.005$) (Fig. 3B-E). However, chromosome segregation was not affected during meiosis (Figure S2). These results indicated that NUP37 may play an important role in the asymmetric division during oocyte maturation.

NUP37 deficiency disturbed embryo developmental competence

To further explore the role of NUP37 in preimplantation embryo development, we injected the mixed *Nup37* siRNAs or NC siRNA into zygotes and further cultured them in G1-plus medium for 4 days. The blastocyst rates were calculated. The results showed that the blastocyst formation rate of the SiNup37 group was significantly lower than the SiNC group ($P = 0.007$) (Fig. 4A-C). Since YAP localization is associated with YAP/TEAD activity and YAP/TEAD signaling plays an important role in embryogenesis, we investigated whether NUP37 deficiency could cause a change in the localization of YAP1. As shown in Fig. 5, YAP1 was mainly located in the nucleus from the 4-cell stage to the morula stage in the SiNC group, whereas it was scattered throughout the cytoplasm in the SiNup37 group. These results showed that NUP37 deficiency would disturb YAP1 shuttle from the cytoplasm to the nucleus, which may result in embryo development arrested in mice.

NUP37 inhibition affected TEAD activity

There are four *Tead* genes (*Tead1-4*) that encode the TEAD proteins in mice. We collected the 2-cell, 4-cell, and 8-cell stage embryos after microinjection of mixed-*Nup37* siRNAs or NC siRNA. qPCR results verified that the expression of *Nup37* was reduced by 76.99% at the 2-cell stage ($P < 0.001$), 95.86% at the 4-cell stage ($P = 0.06$), and 71.63% at the 8-cell stage ($P = 0.01$). Comparatively, *Yap1* expression was not reduced at the 2-cell and the 4-cell stages, but it was insignificantly reduced by 31.51% at the 8-cell stage ($P = 0.336$) after *Nup37* knockdown. However, the expressions of *Tead1*, *Tead2*, *Tead4* (YAP1 coactivators) decreased to different degrees at the 4-cell and the 8-cell stages. Compared with SiNC group, *Tead1* expression level was reduced by 53.30% ($P = 0.425$) and 54.36% ($P = 0.079$), *Tead2* expression level was reduced by 62.02% ($P = 0.007$) and 61.00% ($P = 0.173$), and *Tead4* expression level was reduced by 71.93% ($P = 0.093$) and 46.20% ($P = 0.04$) at the 4-cell and the 8-cell stages, respectively (Fig. 6A-F). *Tead3* expression level did not decrease at any stage, and it was consistent with the previous study that stated TEAD3 was undetectable during early embryo development, and *Tead3* $^{-/-}$ mice were apparently normal[28].

Discussion

Our study showed NUP37 highly expressed in both human [13] and mouse oocytes and implicated the potential role of maternally expressed NUP37 in oocyte maturation. As a conserved protein, the expression pattern of NUP37 in mice was similar to humans. *Nup37* knockdown in mice did lead to aberrant PB1 extrusion and some oocytes even displayed "2-cell like" symmetric cleavage. Spindle migration and PB1 extrusion are essential for oocyte quality and embryo developmental competency, and some NUPs are important for meiosis and asymmetric cell division. For example, NUP35 inhibition leads to defective kinetochore-microtubule (K-MT) attachment and PB1 extrusion [7], and ALADIN is important for meiotic spindle assembly and positioning in mouse oocytes [8]. Combined with the evidence of NUPs acting on spindle positioning and our observation of aberrant PB1 extrusion after NUP37 depletion, NUP37 may be involved in spindle migration. However, how NUP37 regulates spindle migration and whether NUP37 depletion leads to female infertility remain further exploring.

YAP is highly expressed in mouse oocytes, and deleting it in oocytes impairs early embryo development [27]. YAP localization was dynamically changed during preimplantation embryogenesis. It was localized to the nuclei of outer cells at the morula stage [29], and localized to the nuclei of trophectoderm (TE) cells in early-stage blastocysts [25], then accumulated at the nuclei of EPI in late-stage blastocysts [30]. YAP1-null embryos show severe developmental defects [27]. The localization of YAP might be regulated by NPCs, and the mechanisms of importation and exportation have been investigated. Phenylalanine-glycine (FG)-rich NUPs limit the passive diffusion of cargoes larger than 40 kDa [31], and β-karyopherins (Kaps) are involved in inducing facilitated transport [32]. Combined with our data, NUP37 might regulate YAP subcellular localization and thus affect embryo developmental competence. Moreover, YAP-TEAD is important in lineage differentiation, and the presence or absence of nuclear YAP regulates *Teads* transcriptional activity. It has been proposed that YAP localization determined the TEAD4 activity and specified the cell fate of TE, and TEAD4 induces *Cdx2* expression prior to blastocyst formation [23–25]. TEAD1 promotes pluripotency, and YAP-TEAD1 is activated and plays an important role in EPI formation [30]. Additionally, TEAD2 is associated with the Oct3/4 promoter, and YAP-TEAD2 signal is involved in embryonic stem cells maintenance and renewal [22, 33, 34]. In the present study, we found that NUP37 depletion also downregulated the expression of *Tead1*, *Tead2*, and *Tead4* at the 4-cell and the 8-cell stages. The decrease in *Teads* expression might be caused by NUP37 inhibition directly or YAP1 mislocalization. We propose that *Tead1*, *Tead2*, and *Tead4* deficiency might influence ICM/TE lineage differentiation, thus reducing the embryo development competency in our study.

Although some maternal genes are essential for oocyte maturation and embryo development in human [35–38], the need for clinical diagnosis in patients with recurrent oocyte maturation defects or IVF failure remains unmet. In vitro experiments and mouse models are tools to provide insight into the potential causes and specific mechanisms of infertility. Our study suggested that NUP37 deficiency might be an underlying cause of recurrent embryonic arrest and provided a potential identification marker of infertility. However, it still needs to be confirmed in clinical cases.

Collectively, we found that the knockdown of NUP37 inhibited YAP shuttle during early embryogenesis, and YAP could no longer transcriptionally activate TEAD as YAP was retained in the cytoplasm. The inhibition of YAP-TEAD activity would ultimately affect embryonic developmental potential.

Supplementary Information The online version contains supplementary material available at https://doi.org/10.1007/s10815-021-02330-x.

Acknowledgements The authors would like to thank Jiaxi Cheng for her careful discussion on the content of the manuscript.

Author contribution Q.G., Q.L., N.W., and A.S. performed the experiments. Q.G. and J.W. analyzed the data. Q.G., Q.L., and L.Y. designed the study. Q.G., Q.L, and L.Y. wrote the manuscript with help from all authors. The manuscript has been approved by all authors for publication.

Funding This work was supported by the National Key Research and Development Program of China (2017YFA0103801) and the National Natural Science Foundation of China (No. 31871447, No. 31571544, and No. 31522034).

Data availability The data underlying this article is available in the article and in its online supplementary material.

Declarations

Ethics approval Animal experimental procedures were followed as the Institutional Animal Welfare and Ethics Committee policies of Peking University (LA2018261).

Conflict of interest The authors declare no competing interests.

References

1. Beck M, Hurt E. The nuclear pore complex: understanding its function through structural insight. Nature reviews Molecular cell biology. 2017;18(2):73–89.
2. Eibauer M, Pellanda M, Turgay Y, Dubrovsky A, Wild A, Medalia O. Structure and gating of the nuclear pore complex. NAT COMMUN. 2015;6(1).
3. Schwartz TU. The structure inventory of the nuclear pore complex. J MOL BIOL. 2016;428(10):1986–2000.
4. Wente SR, Rout MP. The nuclear pore complex and nuclear transport. CSH PERSPECT BIOL. 2010;2(10):a562.
5. Preston CC, Storm EC, Leonard RJ, Faustino RS. Emerging roles for nucleoporins in reproductive cellular physiology (1). Can J Physiol Pharmacol. 2019;97(4):257–64.
6. Angelo MAD, Hetzer MW. Structure, dynamics and function of nuclear pore complexes. TRENDS CELL BIOL. 2008;18(10):456–66.
7. Chen F, Jiao X, Zhang J, Wu D, Ding Z, Wang Y, et al. Nucleoporin35 is a novel microtubule associated protein functioning in oocyte meiotic spindle architecture. EXP CELL RES. 2018;371(2):435–43.
8. Carvalhal S, Stevense M, Koehler K, Naumann R, Huebner A, Jessberger R, et al. ALADIN is required for the production of fertile mouse oocytes. MOL BIOL CELL. 2017;28(19):2470–8.
9. Arafah K, Lopez F, Cazin C, Kherraf ZE, Tassistro V, Loundou A, et al. Defect in the nuclear pore membrane glycoprotein 210-like gene is associated with extreme uncondensed sperm nuclear chromatin and male infertility: a case report. HUM REPROD. 2021;36(3):693–701.
10 Smitherman M, Lee K, Swanger J, Kapur R, Clurman BE. Characterization and targeted disruption of murine Nup50, a p27(Kip1)-interacting component of the nuclear pore complex. MOL CELL BIOL. 2000;20(15):5631–42.
11 Okita K, Kiyonari H, Nobuhisa I, Kimura N, Aizawa S, Taga T. Targeted disruption of the mouse ELYS gene results in embryonic

death at peri-implantation development. GENES CELLS. 2004;9(11):1083–91.
12. Wu X, Kasper LH, Mantcheva RT, Mantchev GT, Springett MJ, van Deursen JM. Disruption of the FG nucleoporin NUP98 causes selective changes in nuclear pore complex stoichiometry and function. Proc Natl Acad Sci U S A. 2001;98(6):3191–6.
13. Yan L, Yang M, Guo H, Yang L, Wu J, Li R, et al. Single-cell RNA-Seq profiling of human preimplantation embryos and embryonic stem cells. NAT STRUCT MOL BIOL. 2013;20(9):1131–9.
14 Asakawa H, Kojidani T, Yang HJ, Ohtsuki C, Osakada H, Matsuda A, et al. Asymmetrical localization of Nup107–160 subcomplex components within the nuclear pore complex in fission yeast. PLOS GENET. 2019;15(6):e1008061.
15 Duan X, Sun SC. Actin cytoskeleton dynamics in mammalian oocyte meiosis. BIOL REPROD. 2019;100(1):15–24.
16 di Pietro F, Echard A, Morin X. Regulation of mitotic spindle orientation: an integrated view. EMBO REP. 2016;17(8):1106–30.
17 Babariya D, Fragouli E, Alfarawati S, Spath K, Wells D. The incidence and origin of segmental aneuploidy in human oocytes and preimplantation embryos. HUM REPROD. 2017;32(12):2549–60.
18. Mishra RK, Chakraborty P, Arnaoutov A, Fontoura BMA, Dasso M. The Nup107-160 complex and γ-TuRC regulate microtubule polymerization at kinetochores. NAT CELL BIOL. 2010;12(2):164–9.
19 Luo X, Liu Y, Feng W, Lei L, Du Y, Wu J, et al. NUP37, a positive regulator of YAP/TEAD signaling, promotes the progression of hepatocellular carcinoma. Oncotarget. 2017;8(58):98004–13.
20 Varelas X. The Hippo pathway effectors TAZ and YAP in development, homeostasis and disease. DEVELOPMENT. 2014;141(8):1614–26.
21. Pocaterra A, Romani P, Dupont S. YAP/TAZ functions and their regulation at a glance. J CELL SCI. 2020133(2).
22 Kaneko KJ, Cullinan EB, Latham KE, DePamphilis ML. Transcription factor mTEAD-2 is selectively expressed at the beginning of zygotic gene expression in the mouse. DEVELOPMENT. 1997;124(10):1963–73.
23 Yagi R, Kohn MJ, Karavanova I, Kaneko KJ, Vullhorst D, DePamphilis ML, et al. Transcription factor TEAD4 specifies the trophectoderm lineage at the beginning of mammalian development. DEVELOPMENT. 2007;134(21):3827–36.
24. Nishioka N, Yamamoto S, Kiyonari H, Sato H, Sawada A, Ota M, et al. Tead4 is required for specification of trophectoderm in pre-implantation mouse embryos. MECH DEVELOP. 2008;125(3–4):270–83.
25 Nishioka N, Inoue K, Adachi K, Kiyonari H, Ota M, Ralston A, et al. The Hippo signaling pathway components Lats and Yap pattern Tead4 activity to distinguish mouse trophectoderm from inner cell mass. DEV CELL. 2009;16(3):398–410.
26 Sha QQ, Zheng W, Wu YW, Li S, Guo L, Zhang S, et al. Dynamics and clinical relevance of maternal mRNA clearance during the oocyte-to-embryo transition in humans. NAT COMMUN. 2020;11(1):4917.
27. Yu C, Ji SY, Dang YJ, Sha QQ, Yuan YF, Zhou JJ, et al. Oocyte-expressed yes-associated protein is a key activator of the early zygotic genome in mouse. CELL RES. 2016;26(3):275–87.
28 Sawada A, Kiyonari H, Ukita K, Nishioka N, Imuta Y, Sasaki H. Redundant roles of Tead1 and Tead2 in notochord development and the regulation of cell proliferation and survival. MOL CELL BIOL. 2008;28(10):3177–89.
29. Gerri C, McCarthy A, Alanis-Lobato G, Demtschenko A, Bruneau A, Loubersac S, et al. Initiation of a conserved trophectoderm program in human, cow and mouse embryos. NATURE. 2020;587(7834):443–7.
30. Hashimoto M, Sasaki H. Epiblast formation by TEAD-YAP-dependent expression of pluripotency factors and competitive elimination of unspecified cells. DEV CELL. 2019;50(2):139–54.
31 Gamini R, Han W, Stone JE, Schulten K. Assembly of Nsp1 nucleoporins provides insight into nuclear pore complex gating. PLOS COMPUT BIOL. 2014;10(3):e1003488.
32 Kapinos LE, Huang B, Rencurel C, Lim RYH. Karyopherins regulate nuclear pore complex barrier and transport function. J CELL BIOL. 2017;216(11):3609–24.
33. Tamm C, Bower N, Anneren C. Regulation of mouse embryonic stem cell self-renewal by a Yes-YAP-TEAD2 signaling pathway downstream of LIF. J CELL SCI. 2011;124(Pt 7):1136–44.
34 Landin-Malt A, Benhaddou A, Zider A, Flagiello D. An evolutionary, structural and functional overview of the mammalian TEAD1 and TEAD2 transcription factors. GENE. 2016;591(1):292–303.
35. Xu Y, Shi Y, Fu J, Yu M, Feng R, Sang Q, et al. Mutations in PADI6 cause female infertility characterized by early embryonic arrest. The American Journal of Human Genetics. 2016;99(3):744–52.
36. Yang P, Yin C, Li M, Ma S, Cao Y, Zhang C, et al. Mutation analysis of tubulin beta 8 classVIII in infertile females with oocyte or embryonic defects. CLIN GENET. 2021;99(1):208–14.
37 Mu J, Wang W, Chen B, Wu L, Li B, Mao X, et al. Mutations in NLRP2 and NLRP5 cause female infertility characterised by early embryonic arrest. J MED GENET. 2019;56(7):471–80.
38. Feng R, Sang Q, Kuang Y, Sun X, Yan Z, Zhang S, et al. Mutations in TUBB8 and human oocyte meiotic arrest. N Engl J Med. 2016;374(3):223–32.